2008:052

MASTER'S THESIS

Correlation Between N-Hexane/Helium Permporometry, Single Gas and Separation Data for MFI Membranes

Danil Korelskiy

Luleå University of Technology

Master Thesis, Continuation Courses
Chemical and Biochemical Engineering
Department of Chemical Engineering and Geosciences
Division of Chemical Technology

2008:052 - ISSN: 1653-0187 - ISRN: LTU-PB-EX--08/052--SE

Luleå University of Technology
Department of Chemical Engineering and Geosciences
Division of Chemical Technology

Master's Thesis

Correlation between n-hexane/helium permporometry, single gas and separation data for MFI membranes

Danil Korelskiy

June 2008

ABSTRACT

Contemporary separation technology of great interest is high quality membranes, possessing high flux and selectivity together with high durability. Supported membranes based on thin MFI zeolite films and graded supports response to the mentioned requirements to a higher extent. To maintain separation efficiency in a high level, powerful fabrication and characterization techniques of membranes are essential. For the last decade, several techniques for characterization of defects have emerged. Of special interest is adsorption-branch permporometry based on measuring the flow of noncondensable gas, e.g. helium, through membrane as a function of the activity of condensable vapour, normally n-hexane or p-xylene.

In the present work, silicalite-1 membranes with a thickness of 500 nm were prepared by using seeding method. After the preparation, membranes were characterized by single gas permeation and n-hexane/helium permporometry and then, tested for separation of a mixture of hexane isomers: n-hexane and 2,2-dimethylbutane (DMB).

The results of the work showed that single gas permeation data cannot be used for membrane quality estimation. No correlation between single gas permeation data and n-hexane/helium permporometry data has been discovered as well as between single gas permeation data and separation data.

The separation experiments showed that the dependence of the separation factor on temperature is quite spontaneous and unpredictable. On the other hand, it was shown that the DMB permeance at room temperature in a n-hexane/DMB mixture can be predicted by permporometry data. Also, an empirical correlation between n-hexane permporometry and the separation data has been found.

Finally, the present work also demonstrated the strength of adsorption branch permporometry for zeolite membrane quality characterization.

Keywords: Correlation, MFI, Membrane, Permporometry, Single gas, Separation.

ACKNOWLEDGEMENTS

First of all, I would like to thank my supervisor, Professor Jonas Hedlund for giving me the opportunity to work on this interesting project and being always open up for discussions and help.

I would like to give my special thanks to my assistant supervisor, M. Sc. Linda Sandström for being my "guardian angel" during the whole this time and lending me a helping hand in everything and every time. It was great working with you!

Professor Sergey Tretyakov is also acknowledged for being such an understanding person and for all the help and support.

Also, I would like to thank all the people at the Department of Chemical Engineering and Geosciences with special thanks to Charlotte Andersson for giving me good advice and helping me.

Further, I would like to give my hugest thanks to Antonina Lobanova and Christian Andersson for everything you have done for me, it's really a lot! Thank you guys for being not just my friends, but my family too!

I also would like to give my deepest thanks to all my friends for your love, support and encouragement. Special thanks go to Ekaterina Petrova for being able to suffer so strange person as I am during 24 hours a day and supporting me all the time.

Finally, I would like give my warmest thanks to my big family and especially, to my mom and my granny. I would never achieve that I have achieved to this moment without you and your love, support and encouragement. Я вас очень *люблю* и вы всегда в моем сердце!

CONTENTS

1 INTRODUCTION

1.1 Background

Currently, membranes play a very important role in separation technology. A new technology of special interest is zeolite membranes due to their high flux and selectivity in combination with chemical and thermal stability. To obtain high flux, membranes should be as thin as possible in order to reduce mass transport resistance. Here, supported membranes, combining thin zeolite film with well defined micropores and a graded support with low mass transport resistance, are the most frequently used. High selectivity, i.e. high separation factor towards one of the components in a mixture, can be achieved only for virtually non-defective membranes. Therefore, a fabrication of virtually perfect membranes is essential and in order to succeed, good techniques for defect characterization are essential. Here, scanning electron microscopy (SEM) and X-ray diffraction techniques are very powerful. However, an internal film structure cannot be non-destructively characterized by SEM. An emerging technique for characterization of flow through defects is adsorption-branch permporometry. It is a simple and non-destructive technique utilized for membrane quality characterization. The method is based on investigation of how the flow of a noncondensable carrier gas (e.g. He) through the membrane depends on the activity of a condensable vapour (normally, n-hexane or p-xylene). We believe that this technique can precisely indicate not only membrane quality but also membrane separation performance.

1.2 Scope of the Present Work

The scope of the present work is to for the first time identify any correlation between n-hexane/helium permporometry data, single gas permeation data and n-hexane/2,2-dimethylbutane separation performance.

2 LITERATURE SURVEY

2.1 Zeolites

2.1.1 General Description

Zeolites are natural minerals or synthetic materials with pore size varying between 0.3 to 1.3 nm [1]. The zeolite framework is made up of a three-dimensional network of $[SiO_4]^{4-}$ and $[AlO_4]^{5-}$ tetrahedrons linked by shared oxygen atoms [2].

In general, the zeolite structure can be represented by the following formula [2]:

$$M_{x/n}\left[\left(AlO_2^-\right)_x\left(SiO_2\right)_y\right]\cdot wH_2O\,, \tag{2.1}$$

where M – a cation of valence n;
w – number of water molecules;
y/x – silicon/aluminium (Si/Al) ratio for the zeolite.

Due to the $[AlO_4]^{5-}$ tetrahedrons, the zeolite framework has a net negative charge which is balanced by mobile cations. The cations can be metal cations such as Na^+, K^+ etc., and also ammonium or alkylammonium cations. These cations can be exchanged for other cations, resulting in ion-exchange capacity of the zeolites.

The Si/Al ratio also has a profound effect on the zeolite properties. Higher aluminum content results in a more hydrophilic zeolite and stronger adsorption of polar molecules.

Nowadays, around 180 zeolite frameworks are known and all of them are assigned with a 3-letter Framework Type Code (FTC) [3]. One of the most studied is the MFI framework represented by the zeolites ZSM-5 and silicalite-1. The Si/Al ratio for silicalite-1 is more than 200 while it for ZSM-5 varies from 10 to 200 [4]. The high ratio is expressed in less hydrophilicity and lower ion-exchange capacity for silicalite-1 compared to ZSM-5.

The MFI framework is shown in Figure 2.1. There are two types of channels (pores) in MFI structure: tortuous – along the a-direction in the crystal with dimensions 5.5×5.1 Å and straight – along the b-direction within the crystal with dimensions 5.6×5.3 Å.

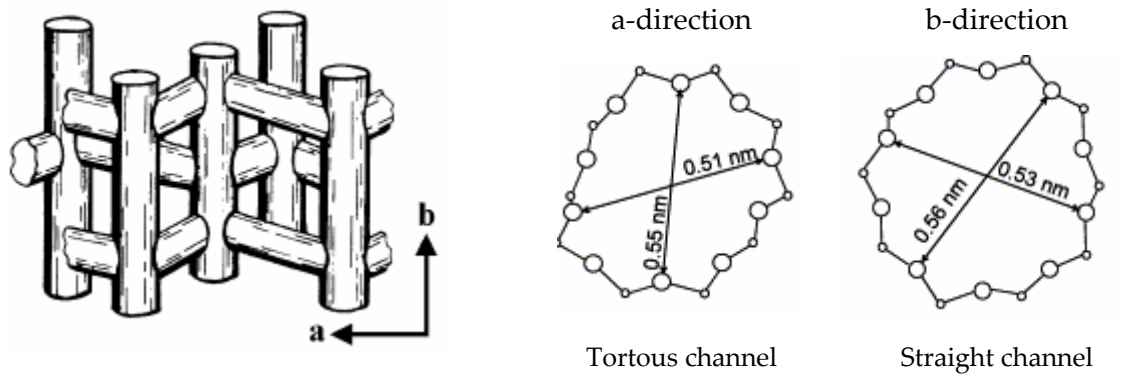

Figure 2.1. MFI-crystal with channel system and crystallographic axes and pore dimensions in a- and b-directions [5].

The small and well-defined pore size provides the zeolites with special features, such as molecular sieving properties. The latter means that zeolites are able to separate different compounds in a blend from each other by molecular size or shape [1].

2.1.2 Zeolite Applications

As mentioned above, zeolites are of great interest for chemical industry and used as ion-exchangers, catalysts, adsorbents and chemical sensors [1, 2, 6, 7].

The ion-exchange capacity provides an opportunity to use zeolites for water purification and effluent treatment. Mainly, zeolites are added to washing powders or detergents to soften the water and here zeolite A is the most applicable [8, 9].

As also known, zeolites have a high catalytic activity and selectivity which makes it possible to use them as catalysts, especially as cracking catalysts (zeolite Y) [2].

Another important feature of the zeolites is their adsorption properties. Due to this fact, zeolites can also be utilized in deep gas dewatering [1], different kinds of purification processes and also for separation of gas and liquid mixtures to its single components by selective adsorption [10, 11].

A novel utilization of zeolite films is chemical sensors. The term "chemical sensor" concerns a device providing insight in the chemical composition of a system [6]. Bjorklund et al. reports [12] that zeolites can be used as additives in order to improve the selectivity and sensitivity of chemical sensors. Grahn et al. [13] reports a new

chemical sensor based on silicalite-1 film which was suitable for hydrocarbons detection at low bulk concentration. Pejcic et al. [14] used zeolite to detect hydrocarbons in gas and liquid phase. Liu et al. [15] utilized zeolites for detection of dissolved organics such as ethanol, propanol and toluene in water. Eventually, zeolites can also be used for organics vapours and water detection in gas phase, especially in air [16].

2.2 Membranes

2.2.1 Introduction

In general, a membrane is defined as a barrier between two phases that provides selective mass transport [17, 18]. Membranes can be prepared from a wide range of solid or liquid organic (normally polymers) and inorganic (carbons, zeolites etc.) materials and membranes may thus be organic or inorganic, natural or synthetic and neutral or charged [17-19].

Currently, membranes and especially solid membranes are of great interest for chemical, pharmaceutical, metallurgy, pulp and paper, automotive, textile and other branches of industry. Membranes are utilized for different separation processes such as membrane gas separation, pervaporation, reverse osmosis, ultrafiltration, microfiltration, hemodialysis, electrodialysis and membrane distillation [17, 19, 20].

At the same time, to be attractive to an industry, membranes must possess at least the following properties: high flux, high selectivity (rejection), mechanical, chemical and thermal stability and eventually low manufacturing cost [18, 20]. Of the above requirements, high flux and selectivity have a profound effect on membrane performance. The combination of these two features determines the extent of separation and the rate of the industrial process. The higher the flux of a membrane, the smaller membrane can be applied, which reduces the costs. Higher selectivity permits a higher separation factor and product purity [18]. Therefore, membranes with a high flux and selectivity are most desirable for separation technology.

All types of membranes can be divided into two groups by their structure: symmetric (isotropic) and asymmetric (anisotropic), see Figure 2.2 [17]. In the first case, the whole membrane structure influences the separation properties of the membrane. The separation properties of anisotropic membranes, on the other hand, are mostly ascertained by the densest region in the membrane. Typically, it is a very thin dense toplayer (thickness is lower than 500 nm). Therefore, this type of membranes exhibits a higher flux and permeation rate compared to symmetric membranes [17, 18].

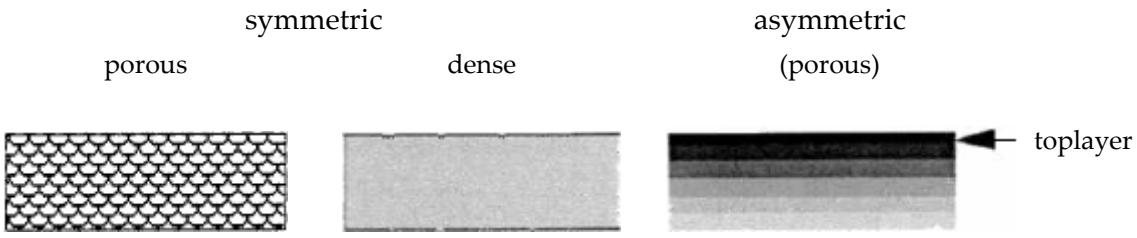

Figure 2.2. Schematic representation of the principal types of membranes [17].

Moreover, membranes can either be classified as porous and dense (homogeneous) [17]. The latter are mainly metal or electrolyte membranes and these materials are highly selective towards hydrogen and various ionic species [21]. However, the industrial interest in dense membranes is much lower compared to porous membranes, which are now playing a leading role in membrane technology [22]. The pores in porous membranes can be categorized according to their shape into straight and tortuous, and by their size into micropores ($d < 2$ nm), mesopores (2 nm $< d < 50$ nm) and macropores ($d > 50$ nm). Accordingly, porous membranes might be microporous, mesoporous and macroporous.

2.2.2 Terminology

The following terms and definitions are important in membrane science: flux, permeance, feed, retentate, permeate, permselectivity (permeance ratio) and separation factor (separation selectivity).

The feed is the stream which is fed to the membrane for separation. During the separation process over the membrane, the feed stream is divided into two streams: retentate and permeate. The flow rejected by the membrane is called retentate. Correspondingly, the stream passing through the membrane is called permeate [17].

The flux is the flow through the membrane per unit area and the permeance can is defined as the flux divided by the partial pressure gradient across the membrane [17]:

$$\Pi_i = \frac{J_i}{\Delta P_i}, \tag{2.2}$$

where J_i – the flux of the component i through the membrane;
ΔP_i – the partial pressure gradient of component i;
Π_i – the permeance of component i.

Furthermore, the ratio between permeances of pure single gases such as H_2, He, CO_2, denotes permeance ratio (ideal selectivity or permselectivity), see equation 2.3. It is commonly used for membrane quality estimation [23].

$$\alpha_{i,j}^{Perm} = \frac{\Pi_i}{\Pi j}, \tag{2.3}$$

where $\alpha_{i,j}^{Perm}$ – permeance ratio;

Π_i, Π_j – permeances of the components *i* or *j* through the membrane.

As mentioned above, the selectivity of a membrane is one of the most important features determining the performance of a given membrane. Typically, the selectivity is characterized by two parameters: the retention and the separation factor (separation selectivity) [17]. The term retention is often used to express the selectivity when separation of dilute aqueous mixtures is carried out over the membrane. The retention is defined as [17]:

$$R = \frac{C_f - C_p}{C_f} = 1 - \frac{C_p}{C_f}, \tag{2.4}$$

where R – the retention;

C_f – the solute concentration in the feed;

C_p – the solute concentration in the permeate.

Therefore, if the retention is equal to 1 or 100 %, complete separation is achieved. It is also clear that there is no separation over a given membrane when the retention is 0.

In the case of gas mixture separation or separation of mixtures of organic liquids, membrane selectivity is generally described by the separation factor defined as [17]:

$$\alpha_{i,j} = \frac{(y_i / y_j)}{(x_i / x_j)}, \tag{2.5}$$

where $\alpha_{i,j}$ – the separation factor;

x_i, x_j – molar fractions (concentrations) of the components *i* and *j* in the feed;

y_i, y_j – molar fractions (concentrations) of the components *i* and *j* in the permeate.

The higher the separation factor towards one of the components, the higher is the membrane selectivity in relation to this component. Obviously, if the separation factor is equal to 1, no separation is reached.

2.2.3 Properties of Zeolite Membranes

Nowadays, a few commercial plants utilizing zeolite membrane technology are operational. Indeed, zeolite membranes can be used for separation of mixtures that may be virtually impossible or very hard to separate by other methods [24]. As mentioned above, zeolites have a narrow pore size distribution and their pore diameter is close to the molecule size of many industrially important organic compounds. Furthermore, zeolite membranes possess pronounced hydrophobic/organophilic adsorption properties. This opens up the powerful potential to separate mixtures by molecular sieving, difference in diffusivities or selective adsorption over the zeolites membranes [24]. Finally, zeolite membranes exhibit high chemical, thermal and hydrothermal stability together with high flux and selectivity [24, 25].

In general, zeolite based membranes can be divided into two groups: self-supported membranes and membranes with a thin continuous zeolite film supported on a porous carrier material (substrate or support) [26]. Self-supported zeolite membranes are symmetric membranes. The thickness of the membranes is usually quite significant to obtain required mechanical stability. Therefore, these membranes have a lower flux compared to the supported membranes with a thin zeolite toplayer. However, self-supported membranes also possess some advantages owing to the lack of substrate. Firstly, there is no leaching effect [27] and support invasion [28] during the synthesis. Secondly, self-supported membranes do not suffer from crack formation due to difference in thermal expansion coefficients between the zeolite and the substrate [29].

Nevertheless, self-supported zeolite membranes are not at the centre of membrane technology attention. Currently, asymmetric membranes based on MFI type zeolites take the leading positions due to their high flux and selectivity combined with substantial mechanical strength. Different techniques for support protection have made it possible to reduce or virtually eliminate support invasion and leaching effect during membrane synthesis. For instance, the two-step support masking procedure developed by Hedlund et al. [30] resulted in a higher flux and selectivity of fabricated membranes [25]. A separation factor of about 230 at 400 °C for a mixture of n-hexane/2,2-dimethylbutane was obtained in that case. At the same time, those membranes exhibited a very high n-hexane permeance of about $6.0 \cdot 10^{-7}$ $\mathrm{mol \cdot m^{-2} \cdot s^{-1} \cdot Pa^{-1}}$. The H_2 per-

meance at room temperature was also rather high of ~ $2.2 \cdot 10^{-5}$ $mol \cdot m^{-2} \cdot s^{-1} \cdot Pa^{-1}$. Moreover, the reproducibility of the fabrication method was almost perfect.

In the whole, three methods for zeolite membrane preparation are commonly used [30]:

a) in-situ crystallization (direct synthesis);

b) vapour phase transport method;

c) seeding method.

In fact, the first one in the represented list is the most spread way of zeolite membrane synthesis. Both self-supported and supported membranes can be fabricated by direct synthesis. The other two techniques are normally used to synthesize supported membranes on different substrates.

At the same time, substrates, as membranes, can be symmetrical and asymmetrical. The latter is built up of two or more layers with different pore size in order to minimize the mass transport resistance. Moreover, the shape of the substrates may also vary. The most spread are flat discs and tubular substrates. Materials used for support making cover a wide range, from metals and oxides to some polymeric materials. Stainless steel, α– or γ–alumina, silica and graphite serve as good examples of materials used for fabrication of porous substrates [31].

An important fact that needs to be mentioned is defect formation in zeolite films and membranes. Any channels or voids with sizes larger than the zeolite pore size may be considered as defects. Depending on the cause of the defect formation, the following kinds of defects are observed:

a) pinholes (non-closed film). This defect can happen due to incomplete seeding or meagre film thickness [30];

b) cracks. Crack formation can be a result of a mismatch in the thermal expansion between the zeolite and the support. Membranes with metal supports suffer from this problem to a higher extent [32, 33].

c) grain boundaries. Open grain boundaries are believed to be caused by a shortage of space to insert another building element between the two growing crystals [34].

It is clear that the amount of defects has to be minimized to achieve a high quality membrane. Otherwise, a membrane will possess high flux but insufficient selectivity.

2.2.4 Separation by Zeolite Membranes

Three main mechanisms of separation over zeolite membranes can be identified: molecular sieving, preferential adsorption and separation due to different diffusivities, see Figure 2.3 [17, 26].

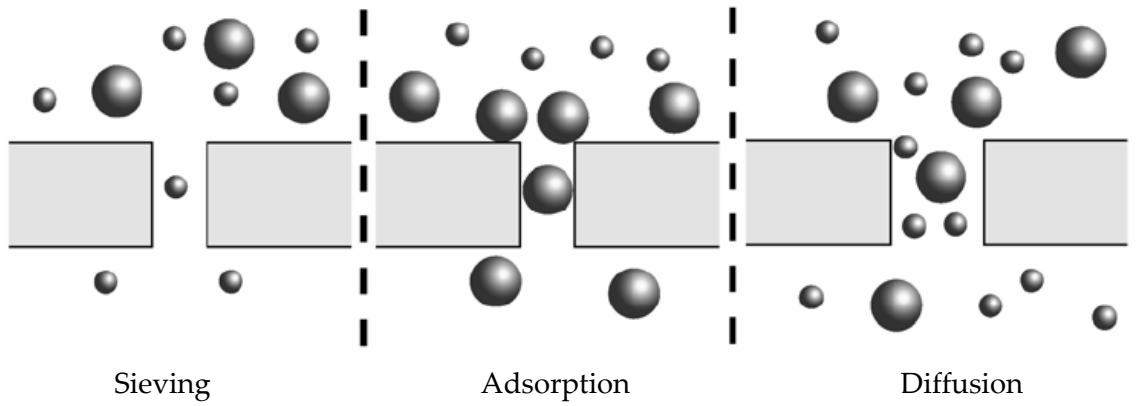

Figure 2.3. Schematic representation of the main types of separation mechanisms [29]

The sieving mechanism provides separation by different size of the molecules. Only molecules smaller than the zeolite pores can pass through the membrane. The larger ones will be rejected by the membrane. In the case of preferential or selective adsorption, there is a component in the mixture which is more strongly adsorbed. As a result, the concentration of this component on the surface is increasing. Therefore, the mass transport of the component through the membrane is also increasing on condition that the molecule size of the component is not larger than the pore size. The last of the mentioned mechanisms is based on differences in diffusivities of the permeating species. Different diffusion rates of species may occur due to differences in molecular weight or size as well as pore size. For instance, if the size of the permeating species is similar to the pore size, then surface diffusion has a profound effect on permeation rate. On the other hand, if the sizes of the permeating species are smaller than the pore size, but the molecules have different molecular weights, then the influence of Knudsen diffusion is very significant [35]. In this case, the permeating molecules collide more with the pore walls than with themselves. A general form of Knudsen diffusion coefficient can be expressed by [36]:

$$D_K = \frac{4}{3} K_0 \sqrt{\frac{8RT}{\pi M}}, \tag{2.6}$$

where D_K – Knudsen diffusivity;
K_0 – structural parameter;
M – molecular weight.

In the event of cylindrical capillaries with the circular pore radius r, D_K may be written as [36]:

$$D_K = 3.068r\sqrt{\frac{T}{M}}\,. \tag{2.7}$$

Knudsen flux of a single component through a channel with radius r can be defined by [36]:

$$J = \frac{F}{A} = -\frac{D_K}{RT}\frac{dP}{dz}, \tag{2.8}$$

where $\frac{dP}{dz}$ – pressure gradient across the membrane.
F – flow of a single component through channels with radius r;
A – area of channels with radius r.

At steady state, an integrated form for the Knudsen flux can be written as:

$$J = \frac{F}{A} = \frac{D_K}{RT}\frac{\Delta P}{\delta}, \tag{2.9}$$

where ΔP – pressure difference across the membrane;
δ – film thickness.

The Knudsen diffusion mechanism normally operates in the range of channels of 10 nm to 100 nm [36].

In fact, the separation process is typically a complex process and all of the three denoted mechanisms can occur simultaneously.

3 EXPERIMENTAL

3.1 Membrane Fabrication

Silicalite-1 membranes with a thickness of 500 nm were fabricated by a technique described in detail earlier [25]. Porous asymmetric α-alumina discs with a diameter of 25 mm were utilized as supports. The supports were previously masked as described earlier [25] and then seeded, before that the supports were submerged in the synthesis solution and heated at 100 °C for 36 h. Colloidal silicalite-1 crystals with a size of 50 nm were used as seeding crystals. The molar composition of the synthesis solution used for film preparation was 3 TPAOH: 25 SiO_2: 1450 H_2O: 100 EtOH. After synthesis, the membranes were calcined at 500 °C for 6 h.

3.2 Permeation Measurements

3.2.1 Single Gas Measurements

Single gas experiments were carried out directly after calcination. The membranes were taken out from the furnace at 110 °C and then immediately mounted in a stainless steel cell. During mounting, a flow of dry nitrogen was used to prevent water adsorption. Rubber gaskets with an inner diameter of 20.3 mm were used during single gas experiments for sealing.

A total pressure gradient was used and the feed pressure was varied from 1.5 bar to 1.9 bar absolute pressure, while the permeate side was kept at atmospheric pressure. The volumetric flow rate of the permeate was measured with an electronic flow meter (ADM 1000 J&W Scientific, max flow rate 1000 ml/min at NTP). The permeance of a single component was then calculated from the flow using equation (2.2). The gases used as probe molecules during the experiments were hydrogen, helium, nitrogen, CO_2 and SF_6.

3.2.2 n-Hexane/Helium Permporometry

As reported earlier [37], adsorption-branch permporometry can be used for characterization of zeolite membranes. By this tool, it is possible to estimate the size and amount of defects in the membranes. A very important feature of the adsorption-branch permporometry is that it is a non-destructive technique [37], hence, the membrane can be used for other purposes after characterization.

The method relies on investigation of how the flow of a noncondensable carrier gas (e.g. He) through the membrane depends on the activity of a condensable vapour (normally, n-hexane or p-xylene). In the case of n-hexane permporometry, the helium flow is measured as a function of relative pressure of n-hexane, varying from 0 to 1. At the beginning of the measurement, only helium passes through the membrane pores and defects. Then, by increasing the relative pressure of n-hexane, the helium permeance is decreasing since more and more pores will be occupied by n-hexane. The relation between the size of the blocked pores and the relative pressure of the hydrocarbon can be found by using the Horvath-Kawazoe (HK) equation (3.1) for micropores [38] and the Kelvin (K) equation (3.2) for mesopores [36].

$$RT\ln\left(\frac{P}{P_0}\right)=\frac{\Delta H_{ADS}}{(d-d_0)}\left[\frac{\sigma^{10}}{9d_0^9}-\frac{\sigma^4}{3d_0^3}-\frac{\sigma^{10}}{9(2d-d_0)^9}+\frac{\sigma^4}{3(2d-d_0)^3}\right], \tag{3.1}$$

$$d_i = 2d - d_s, \tag{3.1a}$$

$$d_0 = \frac{d_s + d_a}{2}, \tag{3.1b}$$

$$\sigma = \left(\frac{2}{5}\right)^{1/6} d_0, \tag{3.1c}$$

where d_i – pore diameter;
d_s – diameter of a surface atom in the zeolite pores;
d_a – diameter of the hydrocarbon molecule;
d – slit pore half width;
σ – zero interaction energy distance;
ΔH_{ADS} – isosteric heat of adsorption;
$\frac{P}{P_0}$ – relative pressure of the hydrocarbon.

$$r_i = \frac{-2\gamma V_m}{RT \ln\left(\frac{P}{P_0}\right)}, \tag{3.2}$$

where r_i – radius of mesopores;
γ – surface tension;
V_m – molar volume.

The Horvath-Kawazoe and Kelvin diameters are normally considered as meniscus diameters due to capillary condensation [36]. However, adsorption of vapours occurs before capillary condensation. Hence, the true pore diameter will be a sum of the meniscus diameter and double adsorbed layer thickness [36]:

$$d_p = d_M + 2t, \tag{3.3}$$

where d_p – the true pore diameter;
d_M – the meniscus diameter given by the Horvath-Kawazoe or the Kelvin equation;
t – the thickness of adsorbed layer given by the Harkins-Jura equation [36]:

$$t = \sqrt{\frac{C}{B - \lg(P/P_0)}}, \tag{3.4}$$

C, B – constants (differ for different adsorbates).

Using equations (3.1), (3.2), (3.3) and (3.4), a pore/defect size corresponding to each relative pressure can be estimated, see Table 3.1.

Table 3.1: Relative pressure of n-hexane and the corresponding pore/defect diameter.

P/P_0	HK-diameter [nm]	K-diameter [nm]	t [nm]	True diameter [nm]
0.01	1.07	–	0.29	1.65
0.023	1.25	–	0.33	1.89
0.13	–	2.00	0.45	2.90
0.22	–	2.59	0.52	3.63
0.44	–	4.77	0.78	6.21
0.75	–	13.86	1.39	16.64

The pore size diameter in MFI is about 0.55 nm [39]. Therefore, according to the data above, all zeolite pores would be blocked already at P/P_0 = 0.01. The He permeance

measured at this relative pressure indicates the permeance through all defects larger than 1.65 nm and reflexes the total amount of defects to a higher extent. The lower the permeance at P/P_0 = 0.01, the lower is the amount of defects larger than 1.65 nm and hence, the higher is membrane quality.

The experimental setup for permporometry is shown in Figure 3.1.

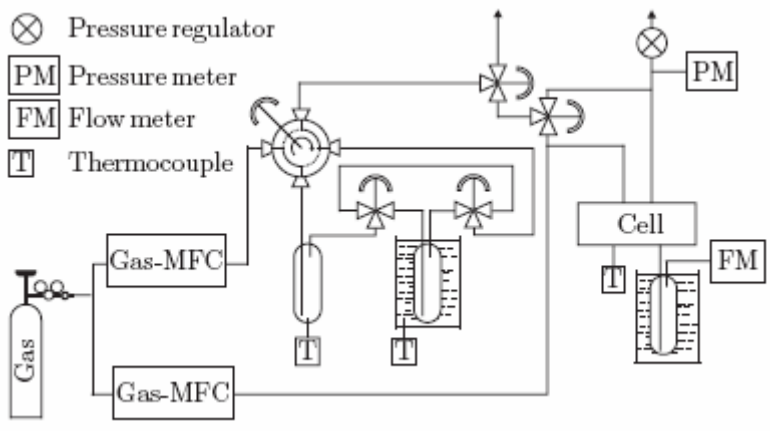

Figure 3.1. Permporometry unit

Before the permporometry experiments, the membranes were mounted in a stainless steel cell and then dried at 300 °C for 6 hours with heating and cooling rate of 1 °C/min. Graphite gaskets with an inner diameter of 19 mm were used for sealing.

The relative pressure of n-hexane was adjusted by two mass flow controllers and then the gas mixture was fed to the membrane in appropriate conditions. At each relative pressure, the system was allowed to equilibrate. The feed side was maintained at 2 bar absolute pressure. The permeate side was always kept at atmospheric pressure. Before the measurement of the permeate, the latter was purified of n-hexane by sending to a condenser connected to the permeate side. Then the volumetric flow rate of the permeated He was measured with an electronic flow meter (ADM 1000 J&W Scientific) and a soap bubble flow meter.

3.2.3 Mixture separation Measurements

A mixture of n-hexane and 2,2-dimethylbutane (DMB) was used as feed in mixture separation experiments. The experiments were carried out in a Wicke-Kallenbach setup, represented in Figure 3.2. In this case, a partial pressure gradient was used as a driving force for diffusion. In order maintain the partial pressure difference, a sweep gas was fed to the permeate side.

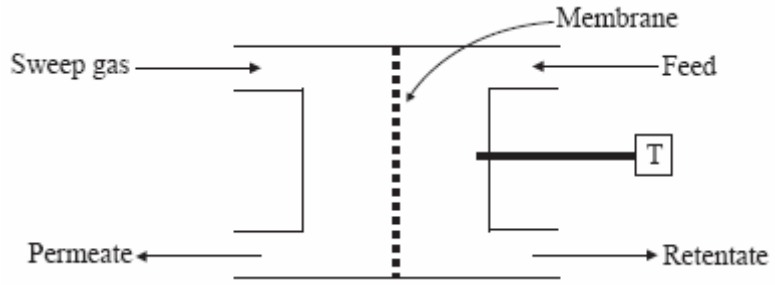

Figure 3.2. Principal setup of a Wicke-Kallenbach cell [36]

The experiments were carried out after the permporometry with the membrane mounted in the same cell. Helium was fed by two mass flow controllers to two saturators maintained at 20 °C by a thermostat. The helium flow to the first saturator, containing 2,2-dimethylbutane, was 100 ml/min and the flow to the second saturator, containing n-hexane, was 280 ml/min. After the saturators, the two streams were mixed and fed to the cell. The feed composition for the separation measurements was thus 11 kPa n-hexane, 11 kPa 2,2-dimethylbutane with helium balance to 100 kPa. Before the measurements, the membranes were always equilibrated with the feed at room temperature. Helium with a flow of 200 ml/min was used as a sweep gas. Schematic representation of a unit used for testing of separation performance is given in Figure 3.3.

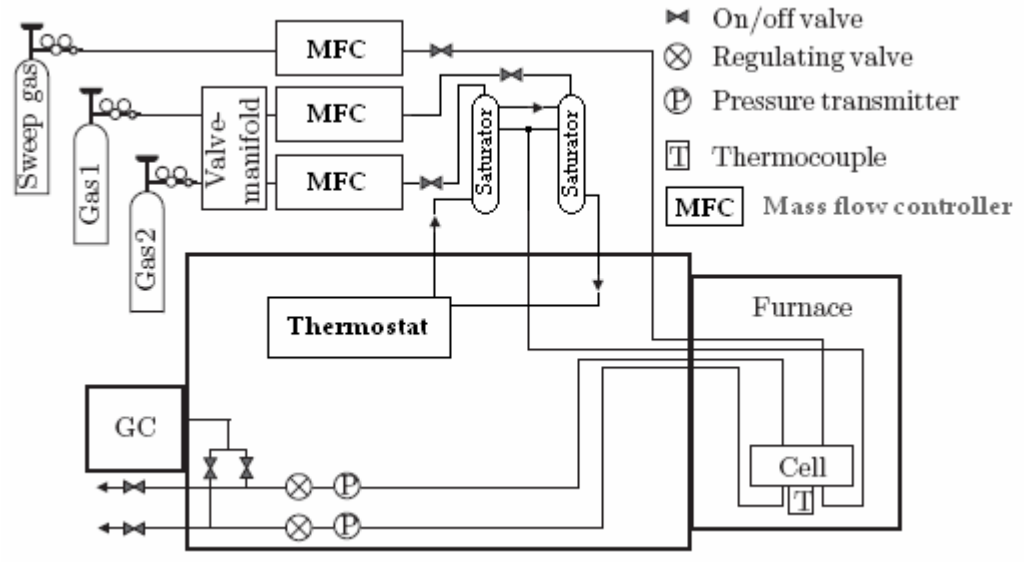

Figure 3.3. Separation performance testing unit

The separation performance has been tested at different temperatures. The first measurements were carried out at room temperature. Then, during the experiment, the membrane was heated up to about 350 °C with a heating rate of 0.5 °C/min.

Analysis of the retentate and the permeate was performed using an on-line gas chromatograph VARIAN chrompack CP-3800.

Eventually, the separation factor was calculated by equation 2.5.

4 RESULTS AND DISCUSSION

4.1 Single Gas Measurements

Single gas permeances and ratios at room temperature for 6 silicalite-1 membranes are represented in Table 4.1. The permeance of small molecules such as H_2, He, N_2 and CO_2 is high, as expected. The permeance of SF_6 is significantly lower. All of the obtained permeances are in a good agreement with those previously reported [25] for similar type of membranes.

Table 4.1: Single gas permeances and ratios at room temperature.

Membrane	Permeance [10^{-7} mol·m^{-2}·s^{-1}·Pa^{-1}]					Permeance ratio				
	H_2	He	N_2	SF_6	CO_2	H_2/He	H_2/SF_6	H_2/CO_2	He/SF_6	N_2/He
Total pressure gradient ΔP = 0.9 bar										
M3	234	106	132	22	168	2.2	10.8	1.4	4.9	1.2
M1	190	79	110	15	144	2.4	13.0	1.3	5.4	1.4
M2	204	89	111	18	143	2.3	11.4	1.4	5.0	1.2
M6	180	76	108	15	147	2.4	12.1	1.2	5.1	1.4
M5	207	88	124	18	161	2.3	11.8	1.3	5.0	1.4
M4	188	77	115	14	164	2.4	13.5	1.2	5.5	1.5
Total pressure gradient ΔP = 0.7 bar										
M3	249	104	129	22	155	2.4	11.1	1.6	4.7	1.2
M1	187	79	109	15	139	2.4	12.2	1.3	5.1	1.4
M2	213	87	113	19	137	2.4	11.0	1.6	4.5	1.3
M6	180	74	108	16	138	2.4	11.5	1.3	4.7	1.5
M5	211	87	120	19	151	2.4	11.2	1.4	4.6	1.4
M4	194	75	117	14	155	2.6	13.4	1.2	5.2	1.6
Total pressure gradient ΔP = 0.5 bar										
M3	240	100	127	24	150	2.4	10.2	1.6	4.2	1.3
M1	187	74	107	16	133	2.5	11.7	1.4	4.6	1.4
M2	200	84	112	19	132	2.4	10.3	1.5	4.3	1.3
M6	176	74	104	17	134	2.4	10.7	1.3	4.5	1.4
M5	204	86	117	19	144	2.4	10.5	1.4	4.5	1.4
M4	191	75	113	15	144	2.6	12.9	1.3	5.0	1.5

According to the data, the permeances of the same probe molecules differ only slightly for all of the tested membranes. This fact roughly indicates a similar quality level of the membranes.

4.2 n-Hexane/Helium Permporometry

Figure 4.1 shows the n-hexane permporometry data for the same 6 silicalite-1 membranes. The first point, at relative pressure of n-hexane equal to 0, corresponds to the permeance of pure He. All membranes exhibit high He permeance, quite close to the He permeance measured in the single gas experiments. Therefore, we can assume that no changes in membrane properties have taken place in between the tests.

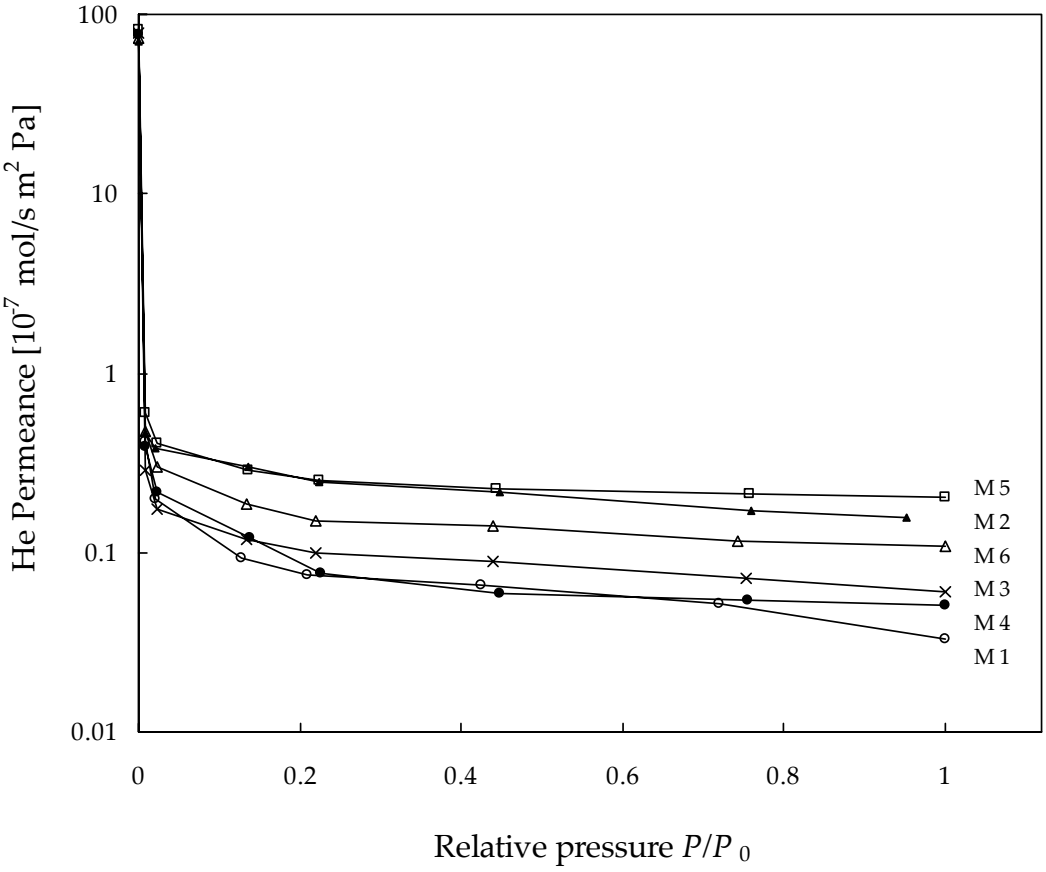

Figure 4.1. n-Hexane permporometry data for siliclite-1 membranes

The He permeance in the relative pressure range $0.01 < P/P_0 < 0.023$ is lower than $1 \cdot 10^{-7}\ \mathrm{mol \cdot m^{-2} \cdot s^{-1} \cdot Pa^{-1}}$ for all of the membranes. The largest He permeance drop is observed in the relative pressure range of 0 to 0.01 and amounts to at least

99.3 % (membrane M5) of the total He permeance. The residual He permeance at a relative pressure of about 1 is lower than $0.1 \cdot 10^{-7}\ \mathrm{mol \cdot m^{-2} \cdot s^{-1} \cdot Pa^{-1}}$, which indicates that the membranes should be free of support cracks. In the whole, all of these observations evidence a very high quality of the membranes.

Furthermore, for membrane M1 a significant drop in the He permeance is also observed in the relative pressure range above 0.72, which indicates a relatively low amount of defects with a diameter larger than 14 nm within the membrane.

Table 4.2 shows the He permeance at relative pressure of 0.01, i.e. via defects larger than 1.65 nm, for tested membranes.

Table 4.2: The He permeance at $P/P_0 = 0.01$

Membrane	He permeance [10^{-8} mol·s^{-1}·m^{-2}·Pa^{-1}]
M3	2.9
M4	3.9
M1	4.1
M2	4.6
M6	4.7
M5	6.1

Membrane M3 would be of highest quality since it has the lowest He permeance at $P/P_0 = 0.01$ and therefore, should exhibit the best separation performance. On the other hand, membrane M5 possesses the highest He permeance via defects larger than 1.65 nm, hence, it is expected to show the poorest separation efficiency.

Figure 4.2 illustrates the permeance ratios: H_2/He, N_2/He and He/SF_6 as a function of the He permeance at $P/P_0 = 0.01$. All of the shown ratios are quite constant and independent of the He permeance at $P/P_0 = 0.01$, i.e. via defects larger than 1.65 nm. The obtained results are in agreement with previously reported by Jareman et al. [40]. This work showed that the permeance ratio mostly depends on substrate morphology, feed pressure, crystallographic orientation and film thickness, rather than some defects. Thus, the minor differences in the observed permeance ratios are believed to be caused only by possible experimental errors or small differences in membrane thickness or substrate morphology. In other words, there is no correlation between the amount of defects estimated by the n-hexane permporometry and the single gas permeation for these not very defective membranes. Therefore, the single gas permeance ratios cannot indicate membrane quality as supposed earlier and, probably, cannot either predict the separation performance.

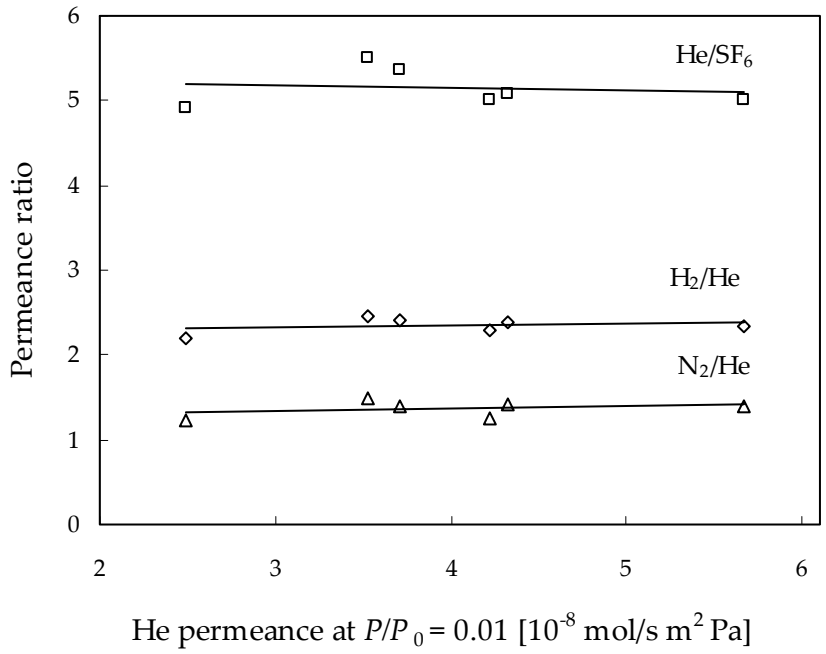

Figure 4.2. Permeance ratio of the tested membranes as a function of He permeance at $P/P_0 = 0.01$

Tables 4.3 and 4.4 show estimated defect distributions for membranes M3 and M5 respectively. The defect distributions were calculated from permporometry data by solving equations (3.1), (3.2), (3.3) and (3.4) (defect distributions for other membranes are shown in Appendix A.2). Knudsen mode of diffusion was assumed as the main diffusion mechanism within the membranes. The area of defects was estimated by solving equations (2.7) and (2.9). Relative area was defined as the area of defects divided by a total membrane area (A_{tot}).

Table 4.3: Defect distribution for membrane M3.

Relative pressure	He permeance [10^{-8} mol·s^{-1}·m^{-2}·Pa^{-1}]	True pore diameter [nm]	Range of defects [nm]	Area of defects [10^{-10} m^2]	Relative area [10^{-3} %]
0	792	-	-	-	-
0.009	2.9	1.65	1.65 – 1.89	54.9	1.94
0.023	1.8	1.89	1.89 – 2.90	20.3	0.71
0.134	1.2	2.90	2.90 – 3.61	4.96	0.17
0.220	1.0	3.61	3.61 – 6.18	1.65	0.06
0.439	0.9	6.18	6.18 – 16.53	1.23	0.04
0.753	0.7	16.53	> 16.53	3.77	0.13
~1	0.6	-	-	-	-

Table 4.4: Defect distribution for membrane M5.

Relative pressure	He permeance [10^{-8} mol·s^{-1}·m^{-2}·Pa^{-1}]	True pore diameter [nm]	Range of defects [nm]	Area of defects [10^{-10} m^2]	Relative area [10^{-3} %]
0	816	-	-	-	-
0.009	6.1	1.66	1.66 - 1.90	94.8	3.34
0.023	4.1	1.90	1.90 - 2.92	42.8	1.51
0.136	2.9	2.92	2.92 - 3.65	9.54	0.34
0.224	2.5	3.65	3.65 - 6.25	4.07	0.14
0.444	2.3	6.25	6.25 - 16.84	0.96	0.03
0.757	2.1	16.84	> 16.84	11.0	0.39
~1	2.0	-	-	-	-

The area of defects is very low for both membranes. At the same time, the defect areas for membrane M5 are around two times higher than the corresponding values for M3. Moreover, the area of defects larger than 16 nm is three times higher for membrane M5 compared to M3.

4.3 Hexane Isomer Separation

4.3.1 n-Hexane/DMB Permeation

After the n-hexane/helium permporometry measurements, the membranes were tested for separation of hexane isomers: n-hexane and 2,2-dimethylbutane (DMB). Figures 4.3 and 4.4 show how permeances of n-hexane and DMB vary with temperature for membranes M3 and M5 respectively (data for the other membranes are shown in Appendix A.3). The n-hexane permeance is more than one order of magnitude higher than the DMB permeance over the entire temperature range. In both cases, the n-hexane permeance is increasing with increasing temperature up to about 60 °C and then decreasing. The DMB permeance for membrane M3 is slightly decreasing over the entire temperature range, while it for M5 goes through a maximum at about 90 °C and then becomes virtually constant.

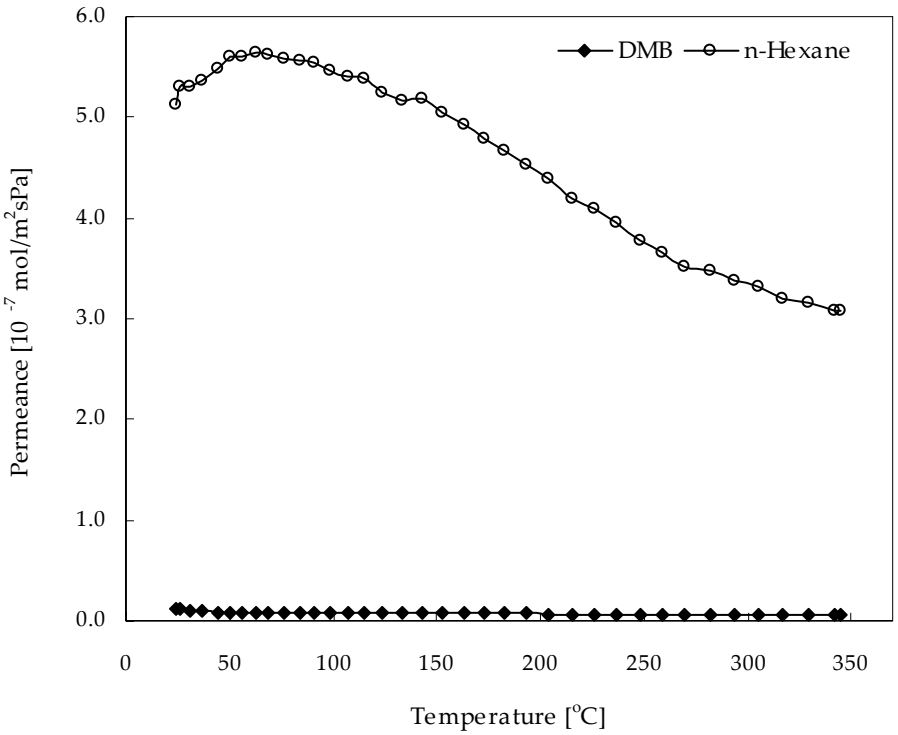

Figure 4.3. Permeance of n-hexane and DMB as a function of temperature for membrane M3

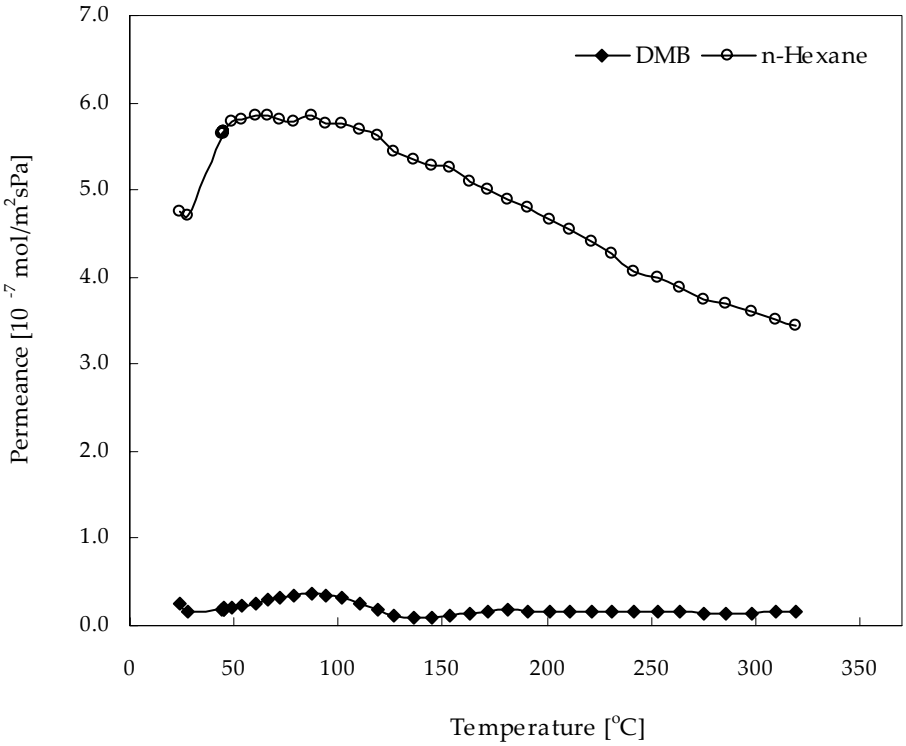

Figure 4.4. Permeance of n-hexane and DMB as a function of temperature for membrane M5

The n-hexane permeance at room temperature for membrane M3 is about $5.1 \cdot 10^{-7}$ mol $\cdot$ m$^{-2} \cdot$ s$^{-1} \cdot$ Pa^{-1}, which is quite close to $5.4 \cdot 10^{-7}$ mol $\cdot$ m$^{-2} \cdot$ s$^{-1} \cdot$ Pa^{-1} that previously reported [25] for high quality membranes of similar type. The DMB permeance at room temperature is about $1.2 \cdot 10^{-8}$ mol $\cdot$ m$^{-2} \cdot$ s$^{-1} \cdot$ Pa^{-1}. Membrane M5 exhibits a slightly lower n-hexane permeance of about $4.8 \cdot 10^{-7}$ mol $\cdot$ m$^{-2} \cdot$ s$^{-1} \cdot$ Pa^{-1}, while the DMB permeance is about $2.6 \cdot 10^{-8}$ mol $\cdot$ m$^{-2} \cdot$ s$^{-1} \cdot$ Pa^{-1}, which is around two times higher than the corresponding value for M3.

According to the literature [24], DMB is diffusing mostly through non-zeolitic pores, i.e. defects, due to a larger kinetic diameter (0.63 nm [41]) compared to the MFI pore size (0.55 nm [24]). The Fickian diffusivity for DMB in the zeolite pores is only around $4.6 \cdot 10^{-20}$ m^2/s [24]. As distinct, the diffusivity for n-hexane is about $3.0 \cdot 10^{-12}$ m^2/s [24]. Therefore, a higher DMB permeance can be expected for more defective membranes. In other words, the DMB permeance is a good indication of membrane quality.

In the separation experiments the total relative pressure of hydrocarbons is about 0.86, which corresponds to the defect size of about 30 nm. Therefore, all defects, smaller than 30 nm should be blocked by n-hexane and most of He and DMB diffuses though defects larger than 30 nm. Thus, the DMB flux at room temperature in the separation experiments would correlate with the He flux at $P/P_0 = 0.86$ in permporometry[1].

Figure 4.5 shows the DMB flux at room temperature in the separation experiments as a function of the He flux at $P/P_0 = 0.86$ in permporometry.

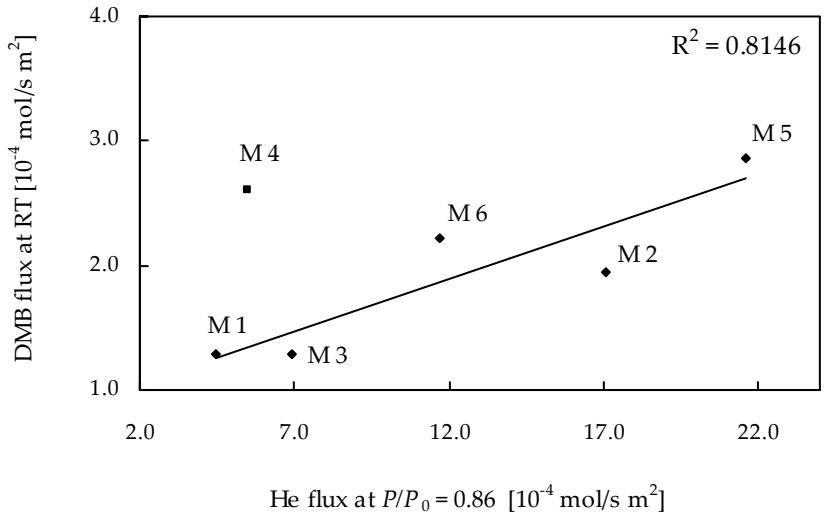

Figure 4.5. The DMB flux as a function of the He flux at $P/P_0 = 0.86$.

[1] A linear interpolation was applied to estimate the He flux at $P/P_0 = 0.86$.

There is a good correlation between the He flux at P/P_0 = 0.86 in permporometry and the DMB flux at room temperature in the separation experiments (R^2 = 0.815). The only exception is membrane M4 which does not fit the correlation and exhibits relatively high DMB flux at relatively low He flux. The reason of this is not clearly understood.

4.3.2 Prediction of DMB Flux

Due to the agreement between permporometry data and the separation data at room temperature, it should be possible to predict the DMB flux from the He flux measured in permporometry. In the case of Knudsen mode as the dominant diffusion mechanism, the DMB flux can be defined by equation (2.8). For the same conditions, owing to equation (2.7), the Knudsen diffusivity for DMB can be related to the He Knudsen diffusivity by:

$$D_k^{DMB} = D_k^{He}\sqrt{\frac{M_{He}}{M_{DMB}}}\,. \tag{4.1}$$

where M_{He} and M_{DMB} – molar weights of He and DMB respectively.

Combining equations (2.7) and (4.1), we get:

$$J_{DMB} = J_{He}\frac{D_k^{DMB}}{D_k^{He}} = J_{He}\sqrt{\frac{M_{He}}{M_{DMB}}}\,. \tag{4.2}$$

Table 4.5 shows the DMB flux calculated by equation (4.2) from the actual He flux at P/P_0 = 0.86 measured in permporometry.

Table 4.5: Predicted DMB flux

Membrane	Actual He flux [10^{-4} mol·s^{-1}·m^{-2}]	Predicted DMB flux [10^{-4} mol·s^{-1}·m^{-2}]	Actual DMB flux [10^{-4} mol·s^{-1}·m^{-2}]	Predicted-to-actual ratio
M3	6.9	1.5	1.3	1.2
M4	5.5	1.2	2.6	0.5
M1	4.5	1.0	1.3	0.7
M2	17.1	3.7	1.9	1.9
M6	11.7	2.5	2.2	1.1
M5	21.6	4.7	2.9	1.6

The predicted-to-actual ratio varies between 0.5 and 1.9. The average predicted-to-actual ratio is 1.2 with standard deviation of ± 0.5 which is very good. Thus, the DMB flux is indeed predictable and can be estimated by using permporometry data.

4.3.3 Separation Performance

The separation factor $\alpha_{Hex/DMB}$ was calculated by equation (2.5). Figures 4.6 and 4.7 show how the separation factor varies with temperature for the membranes. The largest separation factor of about 130 was reached at 215 °C for membrane M1. The lowest factor of about 8 was observed for membrane M6 at 95 °C. In fact, the dependence of the separation factor on temperature is rather chaotic and unpredictable. Obviously, the membrane separation performance is mostly affected by the amount of defects. However, it can also be affected by other parameters such as diffusion mechanism, adsorption processes, film thickness and substrate morphology, thermal stability etc. It is virtually impossible to keep the parameters at the same level with varying temperature even if they vary very slightly for different membranes from the beginning. Moreover, crack formation and coke formation can also occur with increasing temperature. Therefore, any correlation between permporometry data and separation data can be expected only for room temperature where all of the parameters are believed to be quite stable and separation performance would be mostly affected by the amount of defects.

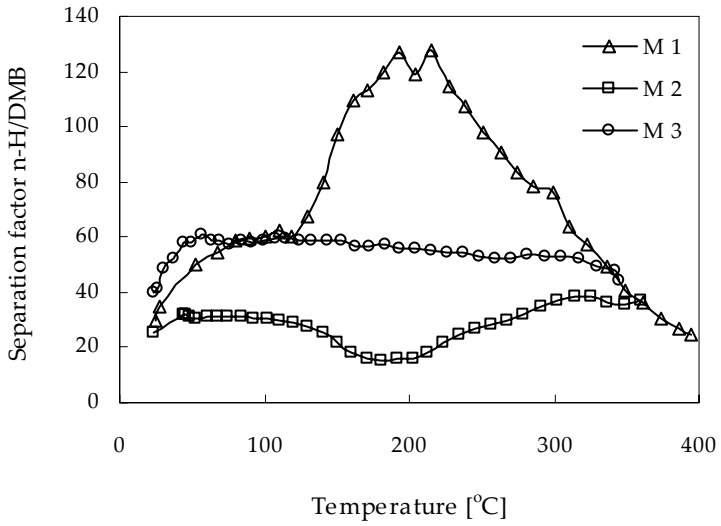

Figure 4.6. Separation factor $\alpha_{Hex/DMB}$ as a function of temperature for membranes M1 – M3

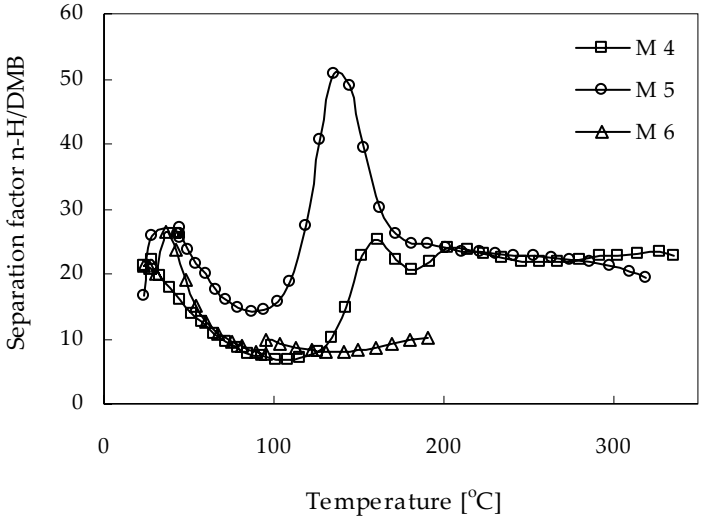

Figure 4.7. Separation factor $\alpha_{Hex/DMB}$ as a function of temperature for membranes M4 – M6

Since the DMB permeance at room temperature is quite predictable and follows the n-hexane/helium permporometry data, we believe that there should be a correlation between the separation factor at room temperature and the He permeance though defects as an index of membrane quality. Figure 4.8 illustrates the separation factor at room temperature as a function of the He permeance at $P/P_0 = 0.01$.

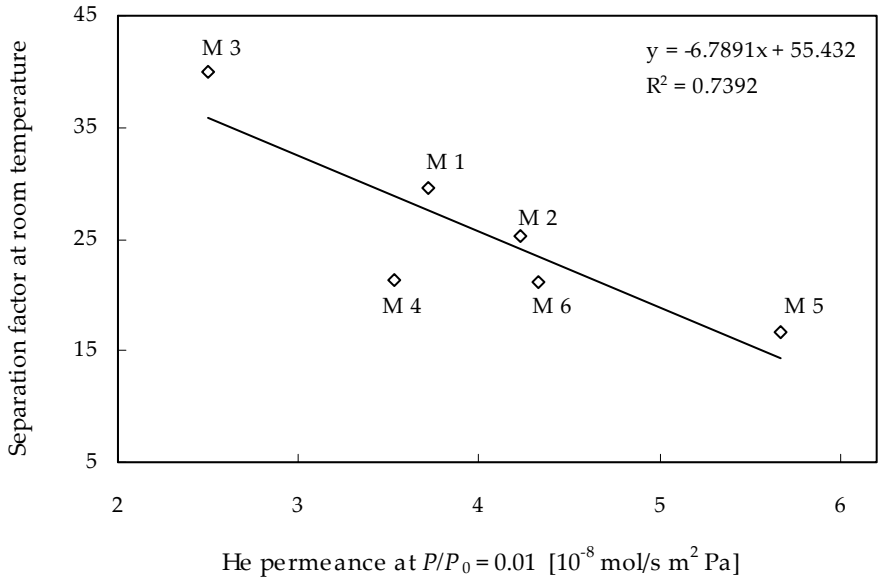

Figure 4.8. Separation factor $\alpha_{Hex/DMB}$ at room temperature as a function of the He permeance at $P/P_0 = 0.01$

There is a correlation (R^2 = 0.74) between the separation performance and the permporometry data for all of the membranes. As expected earlier, membrane M3 exhibits the highest separation factor and M5 – the lowest one. The empirical relation between the He permeance at P/P_0 = 0.01 ($\Pi_{0.01}^{He}$) and the separation factor at room temperature can then be written as:

$$\alpha_{Hex/DMB} = -67.891\Pi_{0.01}^{He} + 55.432\,. \tag{4.4}$$

Therefore, the separation factor can currently be predicted only by equation (4.4) and value of the He permeance at P/P_0 = 0.01. Table 4.6 shows the actual separation factor at room temperature, the separation factor predicted by equation (4.4) and relative error between them.

Table 4.6: Actual separation factor at room temperature, predicted separation factor and relative error between them

Membrane	He permeance [10^{-8} mol·s^{-1}·m^{-2}·Pa^{-1}]	Actual separation factor	Predicted separation factor	Relative Error [%]
M3	2.9	40.0	35.8	10.6
M4	3.9	21.3	28.8	-35.1
M1	4.1	29.5	27.5	6.7
M2	4.6	25.2	24.0	4.6
M6	4.7	21.1	23.3	-10.6
M5	6.1	16.6	14.3	14.0

For five of six membranes the relative error in prediction of the separation factor is less than 15 %. Therefore, adsorption-branch permporometry can be used not only for membrane quality estimation but, also for prediction of membrane separation performance.

Figure 4.9 shows the single gas permeance ratios as a function of the separation factor at room temperature for all of the membranes.

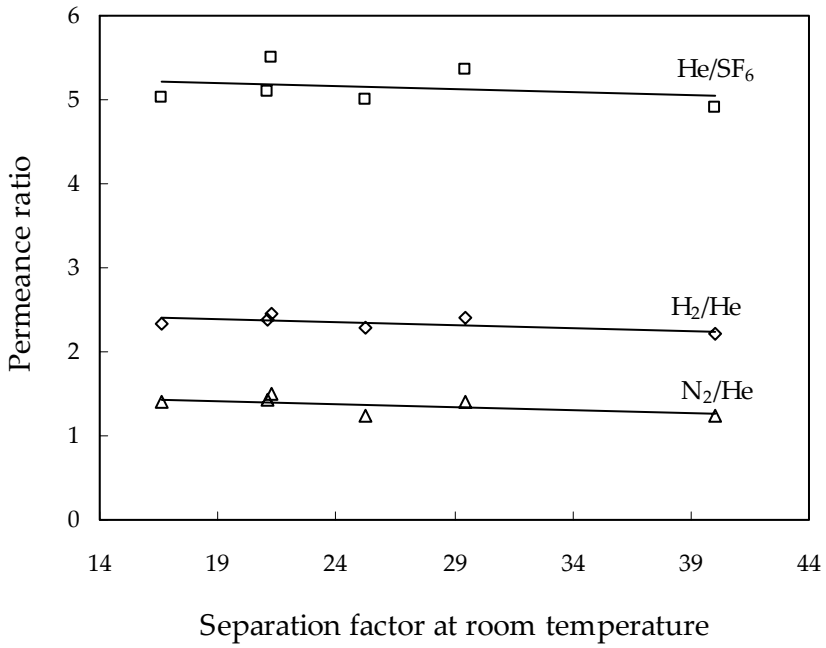

Figure 4.9. Permeance ratios as a function of the separation factor $\alpha_{Hex/DMB}$ at room temperature

There is no any correlation between single gas permeation and separation performance. A lack of correlation between single gas permeation and adsorption-branch perm-porometry data was also shown in Figure 4.2. Hence, in the case of virtually non-defective membranes, single gas permeation analysis cannot be used for prediction of membrane separation performance or membrane quality estimation.

5 CONCLUSIONS

Six silicalite-1 membranes of high and similar quality were prepared and tested in order to investigate the correlation between adsorption-branch permporometry, single gas permeation and separation performance.

The results showed that single gas permeation data cannot be used to estimate quality and separation performance of MFI membranes.

It was shown that the DMB permeance at room temperature in a n-hexane/DMB mixture can be estimated from permporometry data. The estimation is based on an assumption that Knudsen mode of diffusion is the dominant transport mechanism within membranes.

An empirical correlation with R^2 of 0.74 between n-hexane adsorption-branch permporometry data and the separation data for MFI membranes was found.

The results of the work also showed that adsorption-branch permporometry is an effective and powerful technique for membrane characterization.

REFERENCES

1. Breck, D.W., *Zeolite molecular sieves : structure, chemistry and use*. Repr., with corrections and revisions ed. 1984, Malabar, Fla.: Krieger Publ. Company. 771.

2. Satterfield, C.N., *Heterogeneous catalysis in industrial practice*. 2. ed. 1996, Malabar, Fla.: Krieger Pub. 554.

3. The International Zeolite Association, S.C., *Atlas of Zeolite framework Types*, URL: http://topaz.ethz.ch/IZA-SC/StdAtlas.htm.

4. Szostak, R., *Molecular sieves : principles of synthesis and identification*. 2. ed. 1998, London: Blackie. xiii, 359.

5. Krishna, R. and R. Baur, *Modelling issues in zeolite based separation processes.* Separation and Purification Technology, 2003. **33**(3): p. 213-254.

6. Janata, J., et al., *Chemical sensors.* Analytical Chemistry, 1998. **70**(12): p. 179R-208R.

7. Ruthven, D.M., *Principles of adsorption and adsorption processes*. 1984, New York: Wiley. 433.

8. Hui, K.S. and C.Y.H. Chao, *Pure, single phase, high crystalline, chamfered-edge zeolite 4A synthesized from coal fly ash for use as a builder in detergents.* Journal of Hazardous Materials, 2006. **137**(1): p. 401-409.

9. Wilsch-Irrgang, A., et al., *Phosphate and other builder systems - a worldwide comparison.* Tenside Surfactants Detergents, 2003. **40**(4): p. 187-189.

10. Ruthven, D.M. and S.C. Reyes, *Adsorptive separation of light olefins from paraffins.* Microporous and Mesoporous Materials, 2007. **104**(1-3): p. 59-66.

11. Vane, L.M., V.V. Namboodiri, and T.C. Bowen, *Hydrophobic zeolite-silicone rubber mixed matrix membranes for ethanol-water separation: Effect of zeolite and silicone*

component selection on pervaporation performance. Journal of Membrane Science, 2008. **308**(1-2): p. 230-241.

12. Bjorklund, R.B., et al., *Vapor adsorption in thin silicalite-1 films studied by spectroscopic ellipsometry.* Journal of Physical Chemistry B, 1998. **102**(12): p. 2245-2250.

13. Grahn, M., et al., *Silicalite-1 coated ATR elements as sensitive chemical sensor probes.* Microporous and Mesoporous Materials, 2005. **81**(1-3): p. 357-363.

14. Pejcic, B., P. Eadington, and A. Ross, *Environmental monitoring of hydrocarbons: A chemical sensor perspective.* Environmental Science & Technology, 2007. **41**(18): p. 6333-6342.

15. Liu, N., et al., *Nanoporous zeolite thin film-based fiber intrinsic Fabry-Perot interferometric sensor for detection of dissolved organics in water.* Sensors, 2006. **6**(8): p. 835-847.

16. Zhou, J., et al., *Zeolite-modified microcantilever gas sensor for indoor air quality control.* Sensors and Actuators B-Chemical, 2003. **94**(3): p. 337-342.

17. Mulder, M., *Basic principles of membrane technology*. 1991, Dordrecht: Kluwer Academic. xii, 363.

18. Pinnau, I., B.D. Freeman, and American Chemical Society. National Meeting, *Membrane formation and modification*. ACS symposium series, 744. 2000, Washington, D.C.: American Chemical Society. xi, 361.

19. Matsuura, T., *Synthetic membranes and membrane separation processes*. 1994, Boca Raton: CRC Press. viii, 467.

20. Noble, R.D. and S.A. Stern, *Membrane separations technology : principles and applications*. Membrane science and technology series, 2. 1995, Amsterdam ; Oxford: Elsevier. 718.

21. Hsieh, H.P., *Inorganic membranes for separation and reaction*. Membrane science and technology series, 3. 1996, Amsterdam: Elsevier. xvii, 591.

22. Humphrey, J.L. and G.E. Keller, *Separation process technology*. 1997, New York ; London: McGraw-Hill. xv, 408.

23. Jareman, F., *Properties and modeling of MFI membranes*. Doctoral thesis / Luleå University of Technology, 2004:11. 2004, Luleå,. 201.

24. Yu, M., et al., *2,2-Dimethylbutane adsorption and diffusion in MFI zeolite.* Microporous and Mesoporous Materials, 2008. **111**(1-3): p. 24-31.

25. Hedlund, J., et al., *High-flux MFI membranes.* Microporous and Mesoporous Materials, 2002. **52**(3): p. 179-189.

26. Jansen, J.C., *Advanced zeolite science and applications*. Studies in surface science and catalysis, 85. 1994, Amsterdam: Elsevier. xv, 691.

27. Geus, E.R., M.J. Denexter, and H. Vanbekkum, *Synthesis and Characterization of Zeolite (Mfi) Membranes on Porous Ceramic Supports.* Journal of the Chemical Society-Faraday Transactions, 1992. **88**(20): p. 3101-3109.

28. Lai, R. and G.R. Gavalas, *Surface seeding in ZSM-5 membrane preparation.* Industrial & Engineering Chemistry Research, 1998. **37**(11): p. 4275-4283.

29. Andersson, C., *Factors affecting MFI membrane quality*. Doctoral thesis / Luleå University of Technology, 2007:41. 2007, Luleå,. 50.

30. Hedlund, J., et al., *A masking technique for high quality MFI membranes.* Journal of Membrane Science, 2003. **222**(1-2): p. 163-179.

31. Lai, W.F., *Low alkaline inverted in-situ crystallized zeolite membrane*. 1998, Exxon Research & Engineering Company: USA. No. 5824617.

32. denExter, M.J., et al., *Stability of oriented silicalite-1 films in view of zeolite membrane preparation.* Zeolites, 1997. **19**(1): p. 13-20.

33. Geus, E.R. and H. Vanbekkum, *Calcination of Large Mfi-Type Single-Crystals .2. Crack Formation and Thermomechanical Properties in View of the Preparation of Zeolite Membranes.* Zeolites, 1995. **15**(4): p. 333-341.

34. Dong, J.H., et al., *Template-removal-associated microstructural development of porous-ceramic-supported MFI zeolite membranes.* Microporous and Mesoporous Materials, 2000. **34**(3): p. 241-253.

35. Xiao, J.R. and J. Wei, *Diffusion Mechanism of Hydrocarbons in Zeolites .1. Theory.* Chemical Engineering Science, 1992. **47**(5): p. 1123-1141.

36. Do, D.D., *Adsorption analysis : equilibria and kinetics*. Series on chemical engineering, 2. 1998, London: Imperial College Press. 892 +.

37. Clark, T.E., et al., *In situ determination of the adsorption characteristics of a zeolite membrane.* Journal of Membrane Science, 2004. **230**(1-2): p. 91-98.

38. Rege, S.U. and R.T. Yang, *Corrected Horvath-Kawazoe equations for pore-size distribution.* Aiche Journal, 2000. **46**(4): p. 734-750.

39. Bekkum, H.v., *Introduction to zeolite science and practice*. 2., completely rev. and expanded ed. Studies in surface science and catalysis, 137. 2001, Amsterdam: Elsevier. xxi, 1062.

40. Jareman, F. and J. Hedlund, *Single gas permeance ratios in MFI membranes: Effects of material properties and experimental conditions.* Microporous and Mesoporous Materials, 2005. **82**(1-2): p. 201-207.

41. Hedlund, J. and F. Jareman, *Texture of MFI films grown from seeds.* Current Opinion in Colloid & Interface Science, 2005. **10**(5-6): p. 226-232.

42. Perry, R.H., D.W. Green, and R.H. Perry, *Perry's chemical engineers' handbook*. 8. ed. 2008, New York: McGraw-Hill. 2732 med var.pag.

43. Mortimer, R.G., *Physical chemistry*. 3rd ed. 2008, London: Academic. cm.

44. Gregg, S.J. and K.S.W. Sing, *Adsorption, surface area and porosity*. 2. ed. 1982, London: Academic Press. xi, 303.

APPENDICES

Appendix A.1: Chemical and Physical Constants and Properties Used in the Present Work

Table A.1: Chemical and physical properties.

Parameter		Reference
γ [N m^{-1}]	$1.843 \cdot 10^{-2}$	[42]
ρ [kg m-3]	655	[42]
ΔH_{ADS} [J mol^{-1}]	$71 \cdot 10^{3}$	[7]
d_s [m]	$2.76 \cdot 10^{-10}$	[38]
d_A [m]	$4.3 \cdot 10^{-10}$	[1]
R [J mol^{-1} K^{-1}]	8.314	[42]
k [J K^{-1}]	$1.38 \cdot 10^{-23}$	[42]
A_{tot} [m^2]	$2.8 \cdot 10^{-4}$	
Kinetic diameter [nm]:		
He	0.218	[43]
Hexane	0.430	[24]
DMB	0.620	[24]
C [Å^2]	16.77	[44]
B [-]	-0.04	[44]
M_{He} [kg mol^{-1}]	0.004	[42]
M_{DMB} [kg mol^{-1}]	0.086	[42]
δ [nm]	500	

Appendix A.2: Defect Distribution Estimation

Table A.2: Defect distribution for membranes M1, M2, M4 and M6.

Mem-brane	Relative pressure	He permeance [10^{-8} mol·s^{-1}·m^{-2}·Pa^{-1}]	True pore diameter [nm]	Range of defects [nm]	Area of defects [10^{-10} m^2]	Relative area [10^{-3} %]
1	2	3	4	5	6	7
M1	0	769	-	-	-	-
	0.009	4.1	1.64	1.64 – 1.88	103	3.64
	0.022	2.0	1.88	1.88 – 2.86	37.5	1.32
	0.129	0.9	2.86	2.86 – 3.51	5.06	0.18
	0.210	0.8	3.51	3.51 – 5.94	1.69	0.06
	0.424	0.7	5.94	5.94 – 14.43	1.18	0.04
	0.722	0.5	14.43	> 14.43	3.06	0.11
	~1	0.3	-	-	-	-
M2	0	701	-	-	-	-
	0.009	4.6	1.65	1.65 – 1.85	39.3	1.39
	0.020	3.8	1.85	1.85 – 2.92	28.0	0.99
	0.136	3.0	2.92	2.92 – 3.65	14.1	0.50
	0.224	2.5	3.65	3.65 - 6.33	4.83	0.17
	0.449	2.2	6.33	6.33 - 17.13	3.42	0.12
	0.761	1.7	17.13	> 17.13	8.69	0.31
	~1	1.6	-	-	-	-
M4	0	768	-	-	-	-
	0.009	3.9	1.66	1.66 - 1.90	84.2	2.97
	0.024	2.2	1.90	1.90 - 2.93	33.6	1.18
	0.138	1.2	2.93	2.93 - 3.67	12.0	0.42
	0.225	0.8	3.67	3.67 - 6.32	2.82	0.10
	0.448	0.6	6.32	6.32 - 16.75	3.50	0.01
	0.756	0.6	16.75	> 16.75	2.82	0.10
	~1	0.5	-	-	-	-
M6	0	735	-	-	-	-
	0.009	4.7	1.65	1.65 - 1.89	83.4	2.94
	0.023	3.0	1.89	1.89 - 2.90	40.5	1.43
	0.134	1.9	2.90	2.90 - 3.61	8.67	0.31
	0.220	1.5	3.61	3.61 - 6.17	1.65	0.06
	0.439	1.4	6.17	6.17 - 15.85	2.01	0.07
	0.744	1.2	15.85	> 15.85	6.33	0.22
	~1	1.1	-	-	-	-

Appendix A.3: Permeances of n-Hexane and DMB in Separation Measurements

Figures A.3.1 – A.3.4 show how the permeance of DMB and n-hexane varies with temperature for membranes M1, M2, M4 and M6 respectively.

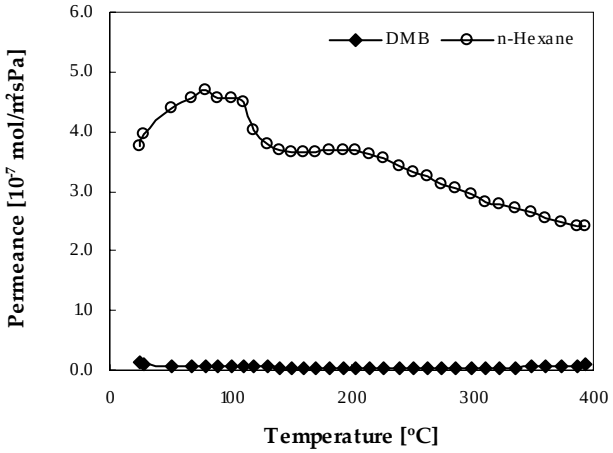

Figure A.3.1. Permeances of n-hexane and DMB vs temperature for membrane M1

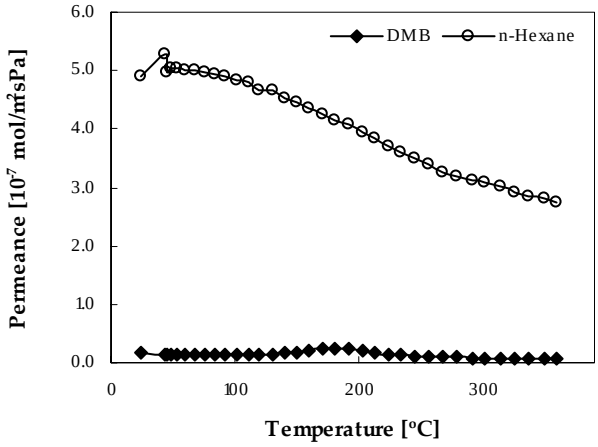

Figure A.3.2. Permeances of n-hexane and DMB vs temperature for membrane M2

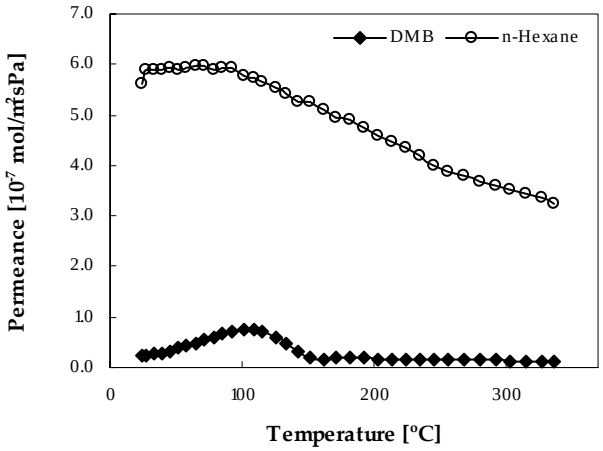

Figure A.3.3. Permeances of n-hexane and DMB vs temperature for membrane M4

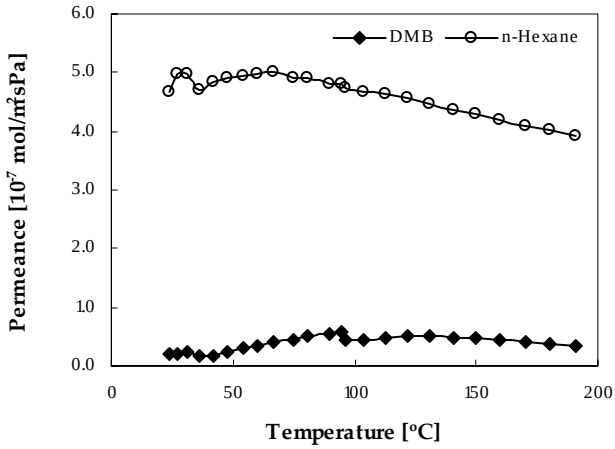

Figure A.3.4. Permeances of n-hexane and DMB vs temperature for membrane M6